Transactions on Electrical and Electronic Materials (2022) 23:254–261
https://doi.org/10.1007/s42341-021-00344-x

Online ISSN 2092-7592
Print ISSN 1229-7607

REGULAR PAPER

Sensitivity Evaluation of a Multi-Layered Heterostructure Blue Phosphorene/MoS_2 Surface Plasmon Resonance Based Fiber Optic Sensor: A Simulation Study

Sachin Singh[1] · A. K. Sharma[2] · Pooja Lohia[3] · D. K. Dwivedi[1]

Received: 28 January 2021 / Revised: 2 May 2021 / Accepted: 7 June 2021 / Published online: 15 June 2021

Abstract
In this study, an angular interrogation technique has been used for modeling a highly sensitive surface plasmon resonance (SPR)based biosensor. The large surface area of the heterostructure of the blue phosphorene (BP/MoS_2) layer facilitates the biomolecules absorption. A four-layer Kretschmann model of the SPR biosensor containing the BP/MoS_2 heterostructure with a gold layer is proposed. Compared to the traditional gold filmbased SPR biosensors, the sensitivity of the proposed SPR biosensor has been significantly improved. An enhanced sensitivity 224.57°/RIU has been achieved by optimizing the proposed structure with 50 nm thick gold layer and a monolayer of heterostructure BP/MoS_2 with a thickness of 0.75 nm. Moreover, the proposed BP/MoS_2 heterostructure offers extremely small FWHM, high detection accuracy, and highquality factor parameters. The highest sensitivity of 252°/RIU was found with two-layers of BP/MoS_2 heterostructure configuration. It is observed that, compared to previously reported sensitivity, the proposed SPR biosensor shows better results.

Keywords Surface plasmon resonance · Heterostructure · 2D nanomaterial · Biosensor · Kretschmann configuration · Sensitivity

1 Introduction

In nano-photonics, plasmonics is a discipline that has played a major role and achieved incredible attention in sensing applications for the last two decades [1]. The concept of surface plasmon resonance (SPR) was reported in 1902, however, the scientific community has not provided a complete explanation of this phenomenon. In 1968, Kretschmann, Raether, and Otto suggested a couple of configurations of plasmon excitement and its concept demonstration [2, 3]. Surface plasmons (SPs) are commonly known as the waves of electron density that propagate at the metal-dielectric interface. Incident photons or electrons are oscillated with free electrons on the metal surface to form a resonance allowing the generation of surface plasmon waves.

The s-polarized light (TE waves) can serve as a reference signal whereas p-polarized light (TM waves) assists the excitation of surface plasmons. Appropriate dispersion diagram indicates that when the horizontal part of the incident light wave-vector K_x (represent the evanescent wave vector) approaches toward the surface plasmon wave-vector (K_{sp}), the SPR arises as:

$$K_X = K_0 n_p \sin\theta_{inc} = K_{sp} \quad (1)$$

where the incident wave vector is denoted by K_0 in free space while θ_{inc} is the angle of incidence, which is also known as the angle of SPR or angle of resonance. It can be observed from the numerical calculations that at 633 nm wavelength of the incident light, by scanning the angle of the incident and monitoring the reflectivity, SPR dip curve is obtained. At the angle of resonance, nearly zero reflectivity is achieved. Some part of optical energy converts into SPW resonance energy during excitation of SPW, which led to a dramatic decrease in the reflected power.

✉ D. K. Dwivedi
todkdwivedi@gmail.com

[1] Amorphous Semiconductor Research Lab, Department of Physics and Material Science, Madan Mohan Malaviya University of Technology, Gorakhpur 273010, India

[2] Department of Applied Sciences, National Institute of Technology Delhi, Narela, Delhi 110040, India

[3] Department of Electronics and Communication Engineering, Madan Mohan Malaviya University of Technology, Gorakhpur 273010, India

For the SPR biosensing angular interrogation process, the SPR angle serves as an effective output signal. The electromagnetic SPR field is redistributed due to changes in the RI (refractive index) of the sensing layer induced by the adsorption of biomolecules to the sensing surface. SPR is a highly sensitive and durable method [4], while there are various sensing methods such as photoluminescence, interferometry, and Doppler effect used for sensing applications. Among all, SPR is an effective technique for real-time detection and has various applications in electrochemistry, life science, environmental safety, and food detection. The main benefit of SPR is that a slight improvement in the RI of the dielectric medium (~ 10^{-7} order) can be observed [5]. It can be divided into three groups (i) surface plasmon (SP) (ii) bulk plasmon, and (iii) localized surface plasmon (LSP) [6]. A prism coupling based SPR sensor working on the concept of attenuated total reflection (ATR) has been explored in several sensing applications [7]. In ATR configuration, according to the principle of energy conversion, the amount of absorption (A), reflectance (R), and transmittance (T) must be equal to unity (i.e., $A+R+T=1$). Assuming no energy loss in addition to material absorption, T is always equal to zero under the ATR condition, so the device absorption can be reduced to $A=1-R$. The reflectance R steadily decreases when the SPs are excited until it reaches a minimum. To obtain the highest SPR performance, the maximum incident light energy is transferred to the evanescent wave [8].

Further, the fiber optic-based sensor has advantages of small size, versatility, low spread loss in single-mode, sensitivity enhancement, and handling of the evanescent area, but it has demerits such as complexity of production, cost, higher multimode spread losses, etc. [9]. While the prism-based SPR sensor has a low multi-mode spread loss, the manufacturing technique is also simple. The metal layers are easily integrated with the flat structure of the prism. Thus, the performance of the prism coupling based SPR sensor is reliable.

Graphene and transition metal dichalcogenides (TMDC) have enormous sensing characteristics such as outstanding mechanical and thermal conductivity, optical transparency, large volume-to-surface ratio. To increase the sensitivity, efficiency factor, and detection accuracy of the SPR sensors, the elevated surface area to volume ratio is very helpful [10–13]. However, researchers are currently concentrating on newly formed 2D nanomaterials such as Blue Phosphorene (BP), Black Phosphorene (BLP), $PtSe_2$, $BaTiO_3$, MXene, and heterostructure 2D nanomaterials. The combination of BP and other 2D materials forming heterostructures have been found as excellent candidates for enhancing the optical and electrical properties, stability, and sensitivity of the material [14].

An updated Kretschmann configuration of the SPR sensor using the Au and heterostructure BP/MoS_2 layer is suggested in this paper to study the impact on performance. We assume that the wavelength of the monochromatic light source is constant (633 nm) while the incidence angle varies. This is recognized as the method of angle interrogation [15]. In this work, sensitivity enhanced SPR sensor configuration employing 2D material such as heterostructure BP/MoS_2 with gold (Au) layer and CaF_2 glass prism has been presented. For the theoretical analysis, we have employed the Fresnel formulation and transfer matrix method (TMM). We observed that the proposed sensor exhibits enhanced sensitivity compared to the conventional gold film based SPR sensor. The optimized sensitivity magnitude of 224.57°/RIU has been obtained in angular interrogation method. Further, the highest sensitivity 252°/RIU is obtained with two layers of heterostructure BP/MoS_2. The reported sensitivity is better than many important studies related to the state-of-the-art (as shown in Table 2).

2 SPR Sensor Structure and Mathematical Modeling

2.1 Structure of the Proposed SPR Sensor

The proposed SPR biosensor is a four-layer system, which is based on Kretschmann configuration (Fig. 1). The particular operating wavelength (633 nm) provides optimum sensitivity along with negligible Kerr effect [16]. BP/MoS_2 heterostructure is directly in contact with the sensing layer and CaF_2 is used as prism whereas Gold (Au) layer is sandwiched between CaF_2 prism and BP/MoS_2 heterostructure.

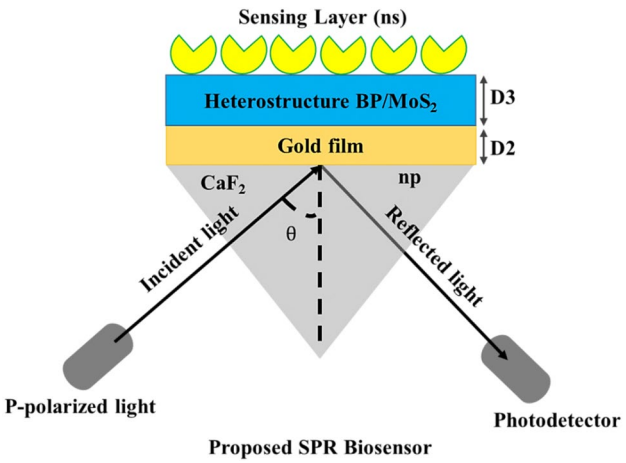

Fig. 1 Proposed device structure of SPR biosensor

2.1.1 First Layer: CaF_2 Prism for Light Coupling

ATR geometry is used for the study of the output resonance curve. The sensitivity of the SPR sensor is also varied with changing the refractive index (RI) of the prism without changing the other parameters [17]. The CaF_2 prism has a low RI ($n_p = 1.4329$) at wavelength 633 nm, which can achieve higher sensitivity [18]. It is found that the refractive index of the prism is an important factor that affects the sensitivity of SPR sensor. The key region is to reduce the n_p value of the glass prism till the resonance position lies in the measurable higher incident angle region and increase the sensitivity of the sensor system. As a result, detection accuracy, quality factor and limit of detection (smallest detectable change in the refractive index of sample) will improve, and much lower concentrations of biomolecules can be detected. Thus, the angular sensitivity of the SPR sensor has enhanced [19]. The optical nonlinearity increases with increased frequency, so light wavelength 633 nm is used. Moreover, the sensitivity of the sensor is improved to the minimum possible Kerr effect at wavelength 633 nm [20].

2.1.2 Second Layer: Metal Layer

In SPR sensors, various transition metals (Au, Ag, Al, Cu, etc.) are used but each metal provides a different performance of the SPR sensor in various ways. Gold (Au) is the most preferred metal due to its good oxidation resistance, stability, higher performance, etc. Au is also a more suitable metal for the generation of SPs because they provide a sharp resonance curve. The RI and dielectric constant (ε_m) of the Au metal layer calculated with help of the Drude-Lorentz model [21] are:

$$n = \sqrt[2]{\varepsilon_m} = \left[1 - \lambda^2\lambda_c \Big/ \lambda_p^2\left(\lambda_c + i\lambda\right)\right]^{1/2} \tag{2}$$

Here λ_c and λ_p are collision and plasma wavelengths having value 8.9342×10^{-6} m and 1.6826×10^{-7} m respectively [22].

2.1.3 Third Layer: Blue Phosphorene/MoS_2

MoS_2 and BP are 2D layer nanomaterials with lattice constants 3.164 Å and 3.268 Å respectively. When these 2D nanomaterials are aligned with strong van der Wall force then it forms a new type of 2D nanomaterial called heterostructure [12]. It is basically combination of conventional 2D nanomaterial (BP) with transition metal dichalcogenides (MoS_2). Heterostructure BP/MoS_2 has higher energy bandgap, work function, charge transfer, mobility and optical absorption compared to conventional 2D nanomaterials. The work function of Au and heterostructure BP/MoS_2 are 5.54 eV and 5.02 eV, respectively [23]. The work function difference causes, the efficiency of charge transfer to the Au layer surface is increased, thus the generation rate of surface plasmons at metal-dielectric interface are increases. Hence the sensitivity of SPR sensor also enhanced. The refractive index (RI) of heterostructure BP/MoS_2 is 2.7915 + 0.355*i at wavelength 633 nm [24, 25].

2.1.4 Fourth Layer: Sensing Medium (1.330–1.340)

For the proposed SPR sensor refractive index of the sensing medium(n_{SM}) is assumed to be n_{SM}=1.330 + Δn, where Δn = 0.002 is the RI shift of the sensing medium with the heterostructure BP/MoS_2 due to the interaction of the biomolecules. When sensing sample contained biomolecules interact heterostructure BP/MoS_2 layer, they are adsorbed on it, contributing to the development of a biomolecular monolayer with modified RI as Δn + 1.330. The RI of the sensing layer is varied from 1.330 to 1.340 for the proposed SPR sensor.

2.2 Mathematical Modeling of Proposed SPR Sensor

In the present study Fresnel equation for multilayer structure and transfer, matrix have been used to investigate the reflectivity of the SPR sensor [26]. To obtain the expression of reflected light intensity of p-polarized light, we consider a multilayer (N-layer) model, and the layers along the z-axis are also thought to be at stake. Each layer has a thickness d_k, permittivity μ_k, refractive index n_k, and dielectric constant ε_k. Here the suffix k represents the prism, metal, heterostructure layer, and sensing medium. The layers are often known to be uniform, isotropic, and non-magnetic. The relation between the tangential field at the initial boundary ($Z = Z_1 = 0$) to the final boundary ($Z = Z_{N\text{-}1}$) is defined as [27]:

$$\begin{pmatrix} P_1 \\ Q_1 \end{pmatrix} = M_{ij} \begin{pmatrix} P_{N-1} \\ Q_{N-1} \end{pmatrix} \tag{3}$$

Here P_1, Q_1, and $P_{N\text{-}1}$, $Q_{N\text{-}1}$ represent a tangential component of the electric and magnetic field at the first and last (Nth) boundary, respectively. The characteristic matrix (M_{ij}) of the combined structure is written as [27]:

$$M_{ij} = \begin{bmatrix} M_{11} & M_{12} \\ M_{21} & M_{22} \end{bmatrix} = \prod_{K=2}^{N-1} M_k \tag{4}$$

where,

$$M_k = \begin{bmatrix} \cos\beta_k & -i\mathrm{Sin}\beta_k/q_k \\ -iq_k\mathrm{Sin}\beta_k & \mathrm{Cos}\beta_k \end{bmatrix} \tag{5}$$

$$q_k = \frac{(\varepsilon_k - n_1^2 \mathrm{Sin}^2\theta)^{1/2}}{\varepsilon_k}, \quad \beta_k = \frac{2\pi d_k}{\lambda}(\varepsilon_k - n_1^2 \sin^2\theta)^{1/2} \tag{6}$$

Here θ and λ are the incident angle and wavelength of the p-polarized light at the base of CaF_2 prism. The value of reflectance (R) for p-polarized light at various incident angles can be calculated with the help of the total reflection coefficient (R_p). Hence reflectance (R) is calculated by $R = \left|R_p\right|^2$, and R_p defines as:

$$R_P = \left[\frac{(M11 + M12qN)q1 - (M21 + M22qN)}{(M11 + M12qN)q1 - (M21 + M22qN)}\right] \tag{7}$$

The performance of the proposed SPR sensor is calculated from SPR curves which depends on various important parameters, such as sensitivity (S), detection accuracy (DA), full width at half maximum (FWHM), and figure of merit (FOM). "MATLAB 2019a" software was used for the simulation results.

3 Performance Parameters of the SPR Sensor

The performance of the SPR sensor depends upon the following three parameters: sensitivity (S), the figure of merit (FOM), detection accuracy (DA) is shown in Fig. 2. The reflectance (R) depends on the variation of RI (Δn) with a change in resonance angle (Δθ) in the sensing medium.

The sensitivity of the SPR sensor is given by [28].

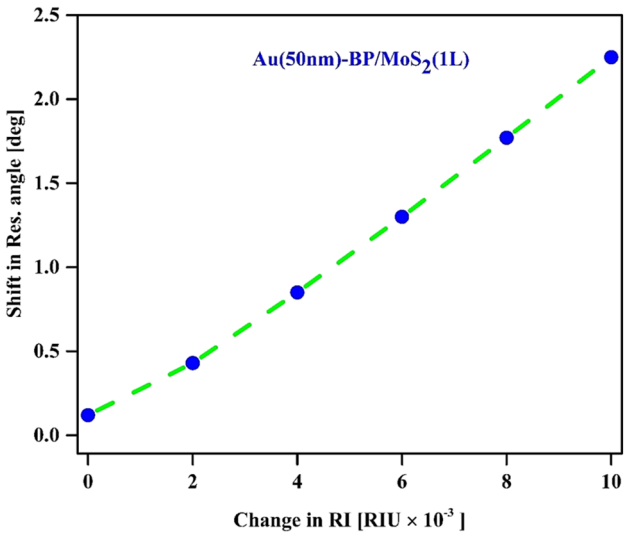

Fig. 2 Change in RI of the sensing layer corresponding change in a shift in resonance angle of proposed SPR biosensor [Au (50 nm)-BP/MoS_2 (1L)]

$$S = \frac{\Delta\theta}{\Delta n} \tag{8}$$

where Δθ and Δn are changing in resonance angle and refractive index respectively.

From the reflectance curve, FWHM is given by:

$$\mathrm{FWHM} = \theta_2 - \theta_1 \tag{9}$$

Here, θ_2 and θ_1 are resonance angles at 50% reflectance measured from the resonance curve.

Detection accuracy (DA) is inversely proportional to FWHM which is given by [28]:

$$\mathrm{DA} = \frac{1}{\mathrm{FWHM}} \tag{10}$$

Quality factor (QF) or figure of merit (FOM) is an important parameter to examine the performance of SPR sensor [28] and given by:

$$\mathrm{QF} = \mathrm{FOM} = \mathrm{S} \times \mathrm{DA} \tag{11}$$

4 Simulation Results and Discussion

4.1 Preliminary Analysis of Gold (Au) Based Conventional SPR Sensing Without Heterostructure of Blue Phosphorene/MoS_2

Figure 3a shows the reflectance curve for RI (n_s) of the sensing medium. The values of RI varying from 1.330 to 1.340 with change $\Delta n = 0.002$ at wavelength 633 nm. Plot 3(a) suggests that sensing possibilities are feasible for a broad range of analytes using the proposed sensor scheme. For n_s values of 1.330–1.340 ($\Delta n_s = 0.002$), the resonance angle (θ_{SPR}) values are 79.02°, 79.41°, 79.82°, 80.23°, 80.66° and 81.01°, respectively. Thus, the average shift of SPR angle ($\Delta\theta_{SPR}$) for conventional SPR sensors is 0.4044°. Therefore, the sensitivity calculation by Eq. (7) reveals that the sensitivity of the conventional SPR sensor is 202.02°RIU^{-1}. FoM and DA values derived from the Eqs. (9) and (10) are 32.188°RIU^{-1} and 0.159 deg^{-1} respectively while Fig. 3b provides the information about the slope and it corresponds to a variation of SPR angle with RI, which also gives the resultant sensitivity of conventional SPR sensor.

4.2 Analysis of SPR Sensing with Heterostructure of Blue Phosphorene/MoS_2

Figure 4a shows the reflectance curve for RI (n_s) of the sensing medium. The values of RI are varying from 1.330 to 1.340 with change $\Delta n = 0.002$ at wavelength 633 nm. Figure 4a illustrates that sensing possibilities are feasible using the proposed sensor system for a wide variety

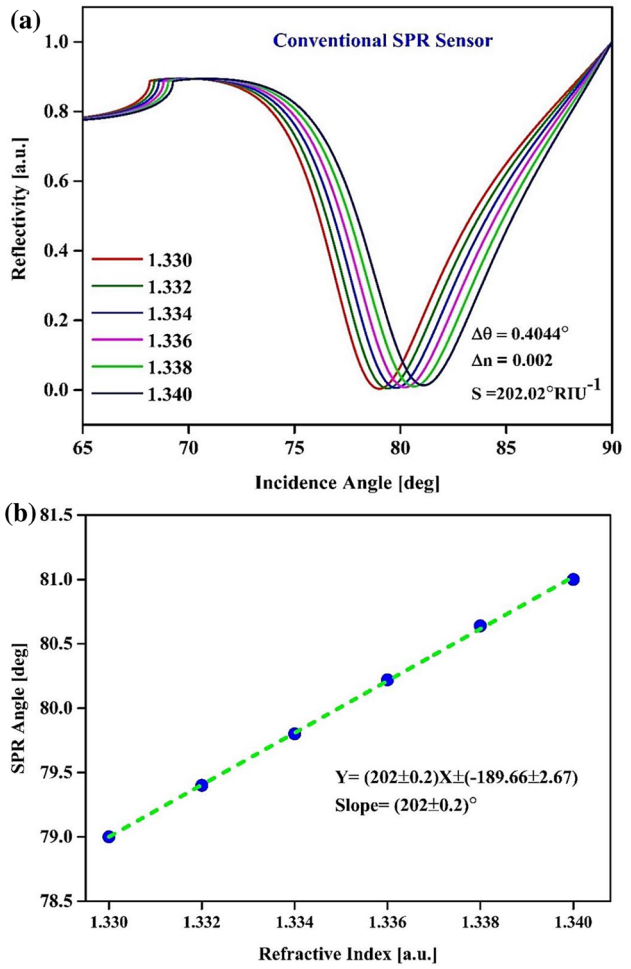

Fig. 3 **a** Represent the reflectance curve **b** Sensitivity variation for conventional SPR sensor

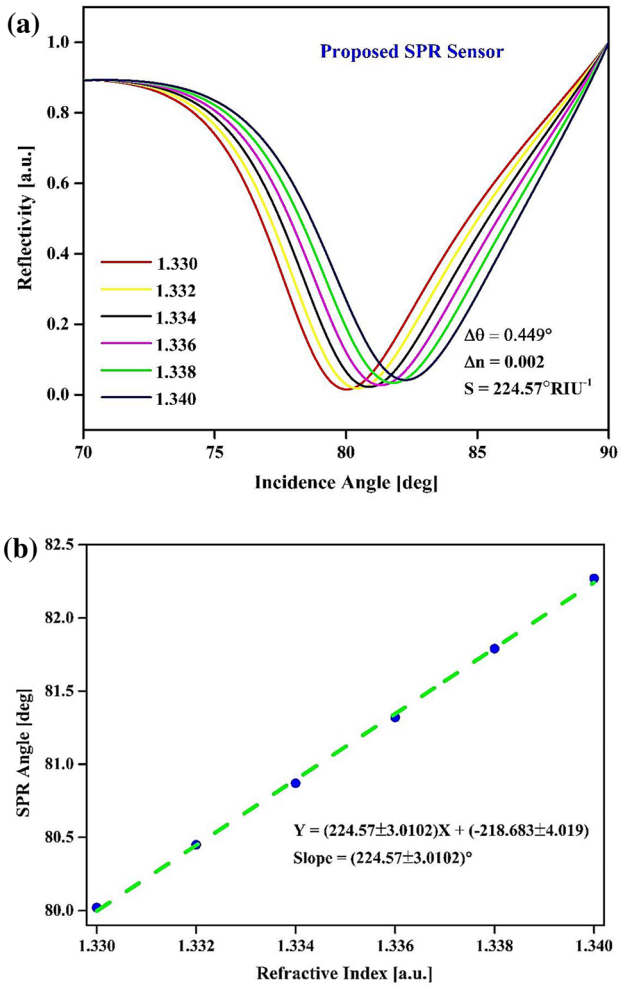

Fig. 4 **a** Represent the reflectance curve **b** sensitivity variation for the proposed SPR sensor

of analytes. For n_s values of 1.330, 1.332, 1.334, 1.336, 1.338 and 1.340, the resonance angle (θ_{SPR}) values are 80.02°, 80.45°, 80.88°, 81.32°, 81.80° and 82.27°, respectively. Thus, the average shift of SPR angle ($\Delta\theta_{SPR}$) for conventional SPR sensors is 0.449°. Therefore, the calculations with Eq. (7) show that the sensitivity of a conventional SPR sensor is 224.57°RIU^{-1}. FoM and DA values derived from the Eqs. (9) and (10) are 36.171°RIU^{-1} and 0.161 deg^{-1} respectively.

Figure 4b provides information about the slope corresponding to the variation of RI with the SPR angle, which also gives the resultant sensitivity of the proposed SPR sensor. After adding 2D material heterostructure BP/MoS_2, the sensitivity of the proposed SPR sensor increases up to 11.2%, due to which overall effective RI increases, thus the shift in resonance angle increases which ultimately results in an increase in FoM as well as DA. Table 1 displays the comparative sensitivity, DA, and FoM review of the traditional SPR biosensor with the proposed SPR biosensor.

4.3 Effect of Increasing the Number of Layers of Heterostructure Blue Phosphorene/MoS_2

Figure 5a shows the variance of the number of layers (B) of the heterostructure BP/MoS_2 at a fixed thickness of 50 nm Au surface, corresponding to the resonance angle changes. As a result, the sensitivity of the proposed sensor also improves. When the number of layers varies, the dip of the reflectance curve is shifted. Thus, the sensitivity, DA, and FoM parameters also change.

From Fig. 5b, the monolayer (B = 0.75 nm) of heterostructure BP/MoS_2 with fixed 50 nm Au layer gives the sensitivity 224.57°RIU^{-1}. Now, we are increasing the thickness of the 2D material layer (d = 0.75 nm x L), where L is the layer thickness of heterostructure BP/MoS_2, then sensitivity also increases up to 252 °RIU^{-1}. Figure 5b, clearly indicates that sensitivity increases (224.57°RIU^{-1}) for 1 layer, becomes maximum (252°RIU^{-1}) at 2 layers and then continually decreases for 5 layers of heterostructure

Table 1 Sensor structures and their performance parameters

SPR sensor structure	Δn	$\Delta\theta_{SPR}$ (deg)	Sensitivity (°RIU^{-1})	FWHM (deg)	DA (deg^{-1})	QF (RIU^{-1})
CaF_2 Prism + Au + Sensing medium (Conventional)	0.002	0.404	202.02	6.2762	0.1593	32.188
CaF_2 Prism + Au + BP/MoS_2 + Sensing medium (Proposed)	0.002	0.449	224.57	6.2091	0.161	36.17

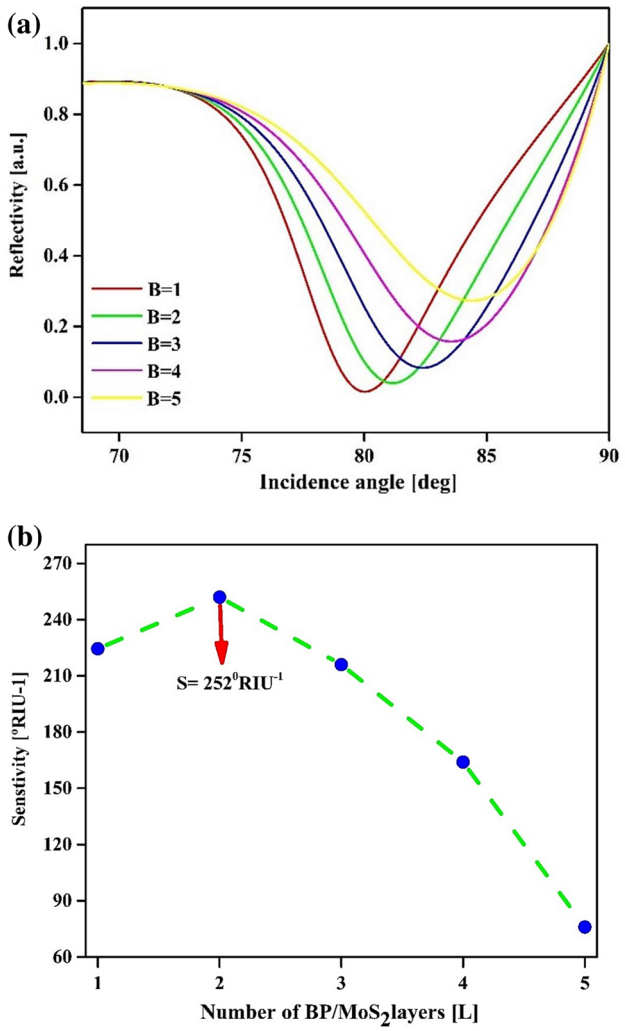

Fig. 5 **a** Reflectivity with incident angle **b** Sensitivity variations with several BP/MoS_2 layers for the proposed SPR sensor

BlueP/MoS_2. The higher carrier confinement, transfer of charge carriers and decreasing of light utilization rate from heterostructure BP/MoS_2 layer to Au layer. The work function difference between BP and MoS_2 nanomaterials also causes the variation of sensitivity. Therefore, the maximum sensitivity 252°RIU^{-1} is optimized for two layers (L = 2) of heterostructure BP/MoS_2 in proposed SPR sensor.

4.4 Effect of Variation with a Thickness of Gold (Au) Layer

Figure 6a displays the variation of reflection with resonance angle by changing thicknesses of the gold layer from 30–65 nm and keeping the thickness of the monolayer heterostructure BP/MoS_2 constant (0.75 nm). By changing several layers, the sensitivity of the proposed sensor increases. Thus, the sensitivity, DA, and FoM parameters also change. From Fig. 6b, it is found that sensitivity increases with increasing metal layer thickness from 30 to 55 nm. Beyond 55 nm layer thickness decrement of sensitivity has been observed. The maximum sensitivity (252°RIU^{-1}) has been observed at 50 nm thickness of the Au layer with two layers (L = 2) of BP/MoS_2, which is in good agreement with recently reported results from other workers. Therefore, we have taken the 50 nm optimum thickness of the Au layer [29, 30].

The optimized sensitivity is found to be much greater for the proposed SPR sensor than all the sensor schemes currently reported and compared in Table 2.

5 Conclusion

This paper introduces a new design for the low RI prism SPR biosensor, heterostructure BP/MoS_2, and Au metal. The proposed sensor shows improved sensitivity compared to the traditional gold film SPR sensor and other reported work. This study optimizes the thickness of the BP/MoS_2 heterostructure layers. The maximum sensitivity of the proposed SPR biosensor is 252°RIU^{-1}, the FWHM is decreased to 6.2091° and the FoM is increased to 36.17°RIU^{-1} in angular interrogation mode because of the optical property components. Our proposed high-sensitivity SPR sensor may a suitable candidate for medical diagnosis and biological applications.

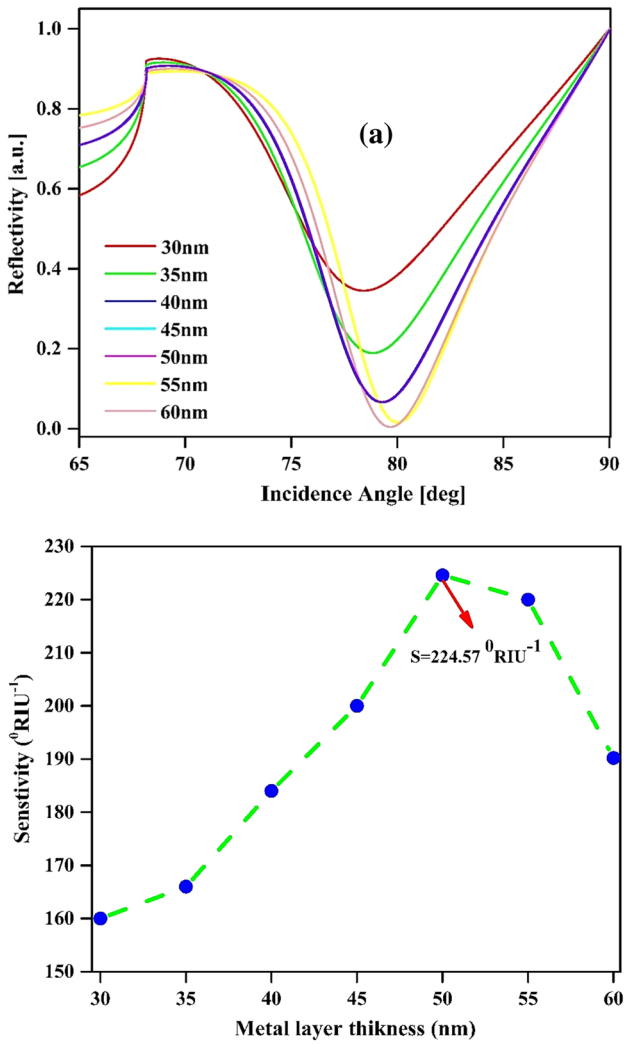

Fig. 6 **a** Reflectance curve shift with incidence angle **b** Variation of sensitivity with metal thickness for the proposed SPR biosensor

Table 2 Comparison of the sensitivity of the proposed sensor with different reported prism-based SPR biosensors

SPR sensor configuration	Wavelength (nm)	Sensitivity	References
Prism/Au/Si/MoS_2/SM	633	131.70	[30]
Prism/Au/MoS_2/Au/G	633	182.0	[31]
Prism/Au/Si/MoS_2/Au/Graphene/SM	633	210.0	[32]
Prism/Au/WS_2/Graphene/SM	633	95.71	[33]
Prism/Au/MoS_2/Ni/Graphene/SM	633	229.0	[34]
Prism/Ag/Franckeite	633	188.0	[35]
Prism/Ag/WS_2/Ni/Graphene/SM	633	243.31	[36]
Prism/Au/heterostructure BP/MoS_2/SM(Proposed)	633	252.0	This study

Acknowledgements One of the authors, Sachin Singh is thankful for the financial assistantship received from MMMUT Gorakhpur, India**.** We are thankful to Dr. Ankit Kumar Panday Department of Electronics and Communications Engineering Bennet University Greater Noida for their valuable suggestions.

Declarations

Conflict of interest The authors confirm that this manuscript has no conflict of interest.

References

1. J.B. Maurya, Y.K. Prajapati, Influence of adhesion layer on performance of surface plasmon resonance sensor. IET Optoelectron. **12**, 168–175 (2018). https://doi.org/10.1049/iet-opt.2018.0008
2. E. Kretschmann, H. Raether, Radiative decay of non radiative surface plasmons excited by light. Z. fur Naturforschung Sect. A J. Phys. Sci. **23**, 2135–2136 (1968). https://doi.org/10.1515/zna-1968-1247
3. A. Otto, Excitation of nonradiative surface plasma waves in silver by the method of frustrated total reflection. Z. Phys. **216**, 398–410 (1968). https://doi.org/10.1007/BF01391532
4. J. Homola, S.S. Yee, G. Gauglitz, Surface plasmon resonance sensors: review. Sens. Actuators B Chem. **54**, 3–15 (1999). https://doi.org/10.1016/S0925-4005(98)00321-9
5. P. Suvarnaphaet, S. Pechprasarn, Graphene-based materials for biosensors: a review. Sensors (Switzerland) (2017). https://doi.org/10.3390/s17102161
6. J. Homola, Present and future of surface plasmon resonance biosensors. Anal. Bioanal. Chem. **377**, 528–539 (2003). https://doi.org/10.1007/s00216-003-2101-0
7. Y.K. Prajapati, A. Yadav, A. Verma et al., Effect of metamaterial layer on optical surface plasmon resonance sensor. Optik **124**, 3607–3610 (2013). https://doi.org/10.1016/j.ijleo.2012.12.021
8. S. Zeng, K.T. Yong, I. Roy et al., A review on functionalized gold nanoparticles for biosensing applications. Plasmonics **6**, 491–506 (2011). https://doi.org/10.1007/s11468-011-9228-1
9. A.A. Rifat, G.A. Mahdiraji, Y.M. Sua et al., Highly sensitive multi-core flat fiber surface plasmon resonance refractive index sensor. Opt. Express **24**, 2485 (2016). https://doi.org/10.1364/oe.24.002485
10. S. Singh, P.K. Singh, A. Umar et al., 2D nanomaterial-based surface plasmon resonance sensors for biosensing applications. Micromachines **11**, 1–28 (2020). https://doi.org/10.3390/mi11080779
11. Ó. Esteban, F.B. Naranjo, N. Díaz-Herrera et al., High-sensitive SPR sensing with Indium Nitride as a dielectric overlay of optical fibers. Sens. Actuators, B Chem. **158**, 372–376 (2011). https://doi.org/10.1016/j.snb.2011.06.038
12. S. Szunerits, N. Maalouli, E. Wijaya et al., Recent advances in the development of graphene-based surface plasmon resonance (SPR) interfaces. Anal. Bioanal. Chem. **405**, 1435–1443 (2013). https://doi.org/10.1007/s00216-012-6624-0
13. C. Zhu, Z. Zeng, H. Li et al., Single-layer MoS2-based nanoprobes for homogeneous detection of biomolecules. J. Am. Chem. Soc. **135**, 5998–6001 (2013). https://doi.org/10.1021/ja4019572
14. Q. Peng, Z. Wang, B. Sa et al., Electronic structures and enhanced optical properties of blue phosphorene/transition metal dichalcogenides van der Waals heterostructures. Sci. Rep. **6**, 2–11 (2016). https://doi.org/10.1038/srep31994
15. J.A. Girón-Sedas, O.N. Oliveira, J.R. Mejía-Salazar, M-Near-Zero metamaterial slabs for a new concept of plasmonic sensing

platforms. Superlattices Microstruct. **117**, 423–428 (2018). https://doi.org/10.1016/j.spmi.2018.03.062
16. J. Park, W.C. Mitchel, L. Grazulis et al., Epitaxial graphene growth by carbon molecular beam epitaxy (CMBE). Adv. Mater. **22**, 4140–4145 (2010). https://doi.org/10.1002/adma.201000756
17. Z. Lin, L. Jiang, L. Wu, J. Guo, X. Dai, Y. Xiang, D. Fan, Tuning and sensitivity enhancement of surface plasmon resonance biosensor with graphene covered Au-MoS2-Au films. IEEE Photonics J. **8**, 1–8 (2016). https://doi.org/10.1109/JPHOT.2016.2631407
18. L. Wu, Y. Jia, L. Jiang et al., Sensitivity improved SPR biosensor based on the MoS2/graphene-aluminum hybrid structure. J. Lightwave Technol. **35**, 82–87 (2017). https://doi.org/10.1109/JLT.2016.2624982
19. G. Gupta, M. Sugimoto, Y. Matsui, J. Kondoh, Use of a low refractive index prism in surface plasmon resonance biosensing. Sens. Actuators, B Chem. **130**, 689–695 (2008). https://doi.org/10.1016/j.snb.2007.10.029
20. J.B. Maurya, Y.K. Prajapati, V. Singh et al., Performance of graphene–MoS2 based surface plasmon resonance sensor using Silicon layer. Opt. Quantum. Electron. **47**, 3599–3611 (2015). https://doi.org/10.1007/s11082-015-0233-z
21. L. Wu, H.S. Chu, W.S. Koh, E.P. Li, Highly sensitive graphene biosensors based on surface plasmon resonance. Opt. Express **18**, 14395 (2010). https://doi.org/10.1364/oe.18.014395
22. A.K. Mishra, S.K. Mishra, R.K. Verma, Graphene and beyond graphene MoS2: a new window in surface-plasmon-resonance-based fiber optic sensing. J. Phys. Chem. C **120**, 2893–2900 (2016). https://doi.org/10.1021/acs.jpcc.5b08955
23. L. Wu, J. Guo, Q. Wang et al., Sensitivity enhancement by using few-layer black phosphorus-graphene/TMDCs heterostructure in surface plasmon resonance biochemical sensor. Sens. Actuators, B Chem. **249**, 542–548 (2017). https://doi.org/10.1016/j.snb.2017.04.110
24. B.D. Gupta, A.K. Sharma, Sensitivity evaluation of a multi-layered surface plasmon resonance-based fiber optic sensor: a theoretical study. Sens. Actuators, B Chem. **107**, 40–46 (2005). https://doi.org/10.1016/j.snb.2004.08.030
25. J. Qiao, X. Kong, Z.X. Hu et al., High-mobility transport anisotropy and linear dichroism in few-layer black phosphorus. Nat. Commun. **5**, 1–7 (2014). https://doi.org/10.1038/ncomms5475
26. K.S. Novoselov, A.K. Geim, S.V. Morozov et al., Two-dimensional gas of massless Dirac fermions in graphene. Nature **438**, 197–200 (2005). https://doi.org/10.1038/nature04233
27. A. Srivastava, Y.K. Prajapati, Performance analysis of silicon and blue phosphorene/MoS2 hetero-structure based SPR sensor. Photonic Sens **9**, 284–292 (2019). https://doi.org/10.1007/s13320-019-0533-1
28. S. Pal, A. Verma, J.P. Saini, Y.K. Prajapati, Sensitivity enhancement using silicon black phosphorous–TMDC coated surface plasmon resonance biosensor. IET Optoelectron. **13**, 196–201 (2019). https://doi.org/10.1049/iet-opt.2018.5023
29. B.A. Sexton, B.N. Feltis, T.J. Davis, Characterisation of gold surface plasmon resonance sensor substrates. Sens. Actuators, A **141**, 471–475 (2008). https://doi.org/10.1016/j.sna.2007.10.020
30. Q. Ouyang, S. Zeng, L. Jiang et al., Sensitivity enhancement of transition metal dichalcogenides/silicon nanostructure-based surface plasmon resonance biosensor. Sci. Rep. **6**, 1–13 (2016). https://doi.org/10.1038/srep28190
31. Z. Lin, L. Jiang, L. Wu et al., Tuning and sensitivity enhancement of surface plasmon resonance biosensor with graphene covered Au-MoS2-Au films. IEEE Photonics J. **8**, 1–8 (2016). https://doi.org/10.1109/JPHOT.2016.2631407
32. K.N. Shushama, M.M. Rana, R. Inum, M.B. Hossain, Sensitivity enhancement of graphene coated surface plasmon resonance biosensor. Opt. Quantum Electron. (2017). https://doi.org/10.1007/s11082-017-1216-z
33. M.S. Rahman, M.R. Hasan, K.A. Rikta, M.S. Anower, A novel graphene coated surface plasmon resonance biosensor with tungsten disulfide (WS2) for sensing DNA hybridization. Opt. Mater. **75**, 567–573 (2018). https://doi.org/10.1016/j.optmat.2017.11.013
34. A. Nisha, P. Maheswari, P.M. Anbarasan et al., Sensitivity enhancement of surface plasmon resonance sensor with 2D material covered noble and magnetic material (Ni). Opt. Quantum Electron. (2019). https://doi.org/10.1007/s11082-018-1726-3
35. S. Gan, Y. Zhao, X. Dai, Y. Xiang, Sensitivity enhancement of surface plasmon resonance sensors with 2D franckeite nanosheets. Results Phys. **13**, 102320 (2019). https://doi.org/10.1016/j.rinp.2019.102320
36. M. Alagdar, B. Yousif, N.F. Areed, M. Elzalabani, Improved the quality factor and sensitivity of a surface plasmon resonance sensor with transition metal dichalcogenide 2D nanomaterials. J. Nanopart. Res. (2020). https://doi.org/10.1007/s11051-020-04872-0